# First Principle Study and Optimal Doping for High Thermoelectric Performance of TaXSn Materials (X = Co, Ir and Rh)

A. Khaldi[1,*], Y. Benallou[1,†], M. Zemouli[2], K. Amara[2], M. El Keurti[2]

[1] *Technology Laboratory of Communication, University of Saida – Dr. Moulay Tahar, 20000 Saïda, Algeria*
[2] *Laboratory of Physico-chemical studies, University of Saida – Dr. Moulay Tahar, 20000 Saïda, Algeria*

In this paper, the full potential linearized augmented plane wave method implemented in the WIEN2K code with first principles-based density functional theory are used to investigate the structural, elastic, electronic and thermoelectric properties of TaCoSn, TaIrSn and TaRhSn. The structural and elastic constants are calculated using the generalized gradient potential developed by Perdew-Burke-Ernzerhof (GGA-PBEsol). The electronic structures are performed by means of GGA-PBEsol and improved by Tran-Blaha modified Becke-Johnson (TB-mBJ) potential. Our results show that the studied compounds are semiconductors with indirect gaps. On the other hand, we investigated the thermoelectric properties at different temperatures with respect to the chemical potential. The results show that the thermopower factors are more important for *p*-type doping than those for *n*-type doping and the maximum value of these factors indicates the optimal hole-doping level which gives rise to high thermoelectric performances of these materials. Finally, we note that the best thermopower values are found for the TaRhSn compound with optimal doping levels of $(75.76, 175.60$ and $238.92) \times 10^{14}$ µW cm$^{-1}$ K$^{-2}$ s$^{-1}$ at temperatures of 300, 600, and 900 K, respectively.

**Keywords:** Semiconductors, Thermoelectric performances, GGA-PBEsol, *p*-type and *n*-type doping levels, Thermopower factors, Doping level.

## 1. INTRODUCTION

At present, with an average yield of about 30 %, most energy resources are consumed as thermal energy. The remaining 70 % is lost and the remainder of this residual energy is emitted as thermal energy to the environment. Although the performance of thermoelectric devices is generally low, they are irreplaceable for certain applications as in the of telecommunications field such as power supply of communication relays or emergency communication systems in remote locations, cooling of detection cells in the infrared, cooling of emission laser diodes used in fiber optic telecommunications, and infrared cameras or thermal imagers, High-performance thermoelectric material research is one of the most important axes of renewable energy sources at present [1], different materials with different crystal structures possess thermoelectric properties such as skutterudite, Clathrates, half-Heusler compounds, Chalcogenides and materials based on complex oxide. These materials are used in thermoelectric devices that have shown great promise in the transfer of waste heat so between the various major heat converters they can directly transform heat into electricity. The efficiency of thermoelectric materials can be characterized by the dimensionless figure of merit $ZT = TS^2\sigma/\kappa$, a quantity in which $S$ is the Seebeck coefficient, $\sigma$ the electrical conductivity, $\kappa$ the thermal conductivity and $T$ the temperature. However, the development of highly efficient thermoelectric materials is still a great challenge sense it requires the decoupling of $\sigma$, $S$ and $\kappa$, which are often unfavorably interdependent according to the Wiedemann-Franz law [2].

Recently, R. Gautier et al. [3] predicted the existence of 18 stable compounds by determining the energy distance in ABX systems. These materials are synthesized and studied by X-ray powder diffraction and transmission electron microscopy (TEM). Among these materials, materials TaXSn (X = Co, Ir and Rh) have been identified as typically single-phase crystalline in the form of a cubic structure of LiAlSi-type with a space group F4-3m. In this paper, we report a theoretical study of the structural, elastic, and electronic properties of TaCoSn, TaIrSn, and TaRhSn semiconductors using the density functional theory (DFT) implemented in the WIEN2k package. On the other hand, by mean of BoltzTraP code [4], the thermoelectric performances of these compounds such as Seebeck coefficient, electrical and thermal conductivity, and thermoelectric power factor with optimal doping concentration are also calculated and discussed in detail at temperature range between 300 and 900 K.

## 2. COMPUTATIONAL DETAILS

We used the calculations of the first principle of the functional density theory (DFT) within the linearized augmented plane wave method (FP-LAPW) [5] implemented in the WIEN2K code [6]. The generalized gradient potential developed by Perdew-Burke-Ernzerhof for solids (GGA-PBEsol) [7] was used to calculate the structural, elastic and electronic properties of the TaCoSn, TaIrSn and TaRhSn compounds. In order to improve the deviations of the prohibited energy bands of the electronic structures, we used the potential of Tran-Blaha's modified Becke-Johnson (TB-mBJ) because it is

---
[*] ahmed.khaldi@univ-saida.dz
[†] benallou06@yahoo.fr

very precise to determine the energy gaps of semiconductors [8]. On the other hand, the BoltzTraP program was employed to determine the thermoelectric properties based on analytical expressions of the electronic bands, which are mounted in Boltzmann's semi-classical model [4].

The atomic radii are taken to be 2.50 for Ta and Sn, 2.00, 2.18 and 2.22 for Co, Rh and Ir respectively, which are chosen so that the muffin-tin spheres do not over-lap. The valence wave functions inside the spheres are extended to the $l_{max} = 10$. The particular choices of muffin-tin radii are made in such a way that the interstitial region between the different atomic spheres is as small as possible to ensure rapid convergence. The cut-off energy corresponds to the $R_{MT} \times K_{max}$ taken to be 8. The integration of the Brillouin zone was conducted using the Monkhorst-Pack mesh [9, 10] of $(15 \times 15 \times 15)$ $k$-points for all compounds. Convergence has been achieved for the total energy in $10^{-5}$ Ry. Finally, to obtain more accurate results for the thermoelectric properties of our compounds, the BoltzTraP code is used with a mesh of $(34 \times 34 \times 34)$ $k$-points.

## 3. RESULTS AND DISCUSSION

### 3.1 Structural Properties

By optimizing their equilibrium energies in the LiAlSi cubic structure with an F4-3m space group, we determined the structural properties of the TaCoSn, TaIrSn and TaRhSn compounds. The structural parameters of these compounds, such as the equilibrium lattice constant ($a$), bulk modulus ($B$) and its pressure derivative ($B'$), were obtained by fitting the total energies as a function of the equilibrium volumes with the Murnaghan state equation [11], given by the following formula:

$$E(V) = E_0 + \frac{BV}{B'}\left[\frac{1}{B'-1}\left(\frac{V_0}{V}\right)^{B'} + 1\right], \quad (1)$$

where $E_0$, $B$, $B'$, and $V_0$ are the energy, the bulk modulus, its pressure derivative, and volume, respectively at equilibrium. The calculated values of structural parameters together with other theoretical and experimental data [3] are listed in Table 1.

**Table 1** – Calculated lattice constant $a$ in (Å), $B$ the bulk modulus (in GPa) and the pressure derivatives of the bulk modulus $B'$ for TaCoSn, TaIrSn and TaRhSn

| Compound | $a$ (Å) | $B$ (GPa) | $B'$ |
|---|---|---|---|
| Our calculations with GGA-PBEsol | | | |
| TaCoSn | 5.901 | 185.00 | 4.64 |
| TaIrSn | 6.182 | 202.82 | 4.61 |
| TaRhSn | 6.137 | 182.69 | 4.76 |
| Other calculations | | | |
| TaCoSn | 5.975[b] | | |
| TaIrSn | 6.175[a], 6.233[b] | | |
| TaRhSn | 6.201[b] | | |

[a] Experimental values [3]
[b] Theoretical Values [3]

The lattice constants of TaCoSn, TaIrSn and TaRhSn are in good agreement with the experimental values and theoretical calculations of Gautier et al [3], due to the success of the GGA-PBEsol potential for optimizing structural properties with the hybrid function of Heyd Scuseria and Ernzerhof (HSE06) [12].

### 3.2 Elastic Properties

The mechanical properties are defined by Taylor's development of the total energy of a system under stress, expressed by the following relation [13, 14]:

$$U(V,\varepsilon) = U(V_0,V) + V_0\left[\sum_i \tau_i \varepsilon_i \xi_i + \frac{1}{2}\sum_{ij} C_{ij}\varepsilon_i \xi_i \varepsilon_j \xi_j\right], (2)$$

where $U(V_0, 0)$ is the energy of the unconstrained system, $V_0$ the equilibrium volume, $\tau_i$ is an element of the stress tensor and $\xi_i$ is a factor which is taken into account by the Voigt index. We adopted the commonly used Voigt-Reuss-Hill (VRH) approximation [15], in which the bulk modulus $B$ and the shear modulus $G$ are defined as follows:

$$B_{VOIGT} = (C_{11} + 2C_{12})/3, \quad (3)$$

$$B_{REUSS} = (3S_{11} + 6S_{12})^{-1}, \quad (4)$$

$$B_{HILL} = 1/2(B_{VOIGT} + B_{REUSS}), \quad (5)$$

$$G_{VOIGT} = (C_{11} - C_{12} + 3C_{44})/5, \quad (6)$$

$$G_{REUSS} = 5(4S_{11} - 4S_{12} + 4S_{44})^{-1}, \quad (7)$$

$$G_{HILL} = 1/2(G_{VOIGT} + G_{reuss}), \quad (8)$$

where $S = C^{-1}$.

In a cubic crystal, the mechanical stability is obtained when the elastic constants ($C_{11}$, $C_{12}$ and $C_{44}$) verify the following conditions [16]:

$$C_{11} - C_{12} > 0, C_{11} > 0, C_{44} > 0, C_{11} + 2C_{12} > 0$$
$$\text{and } C_{12} < B < C_{11} \quad (9)$$

The calculated values of these parameters and the elastic constants are summarized in Table 2 where it can be clearly seen that the conditions of the mechanical stability given by the relations (9) are well verified for TaCoSn, TaIrSn and TaRhSn compounds in the cubic phase of LiAlSi. We can also define the $B/G$ ratio proposed by Pugh [17], which is an index of ductility and fragility of a material. Indeed, if Pugh ratio is less than or equal to 1.75 then the material is brittle. Our calculated $B/G$ ratios are 1.68 for TaCoSn which is at the limit of fragility and 2.22 and 2.45 for TaIrSn and TaRhSn

respectively which indicates that these two compounds are ductile. Note that the ductility decreases from TaRhSn to TaIrSn to TaCoSn. Another important factor,

which is Young module $E$, given by the expression:

$$E = 9BG / (3B+G) . \qquad (10)$$

**Table 2** – The calculated elastic constants $C_{11}$, $C_{12}$, $C_{44}$ (in GPa), shear moduli $G_V$, $G_R$ and $G_H$ (in GPa), Young modulus $E$ (in GPa), Poisson ratio ($v$), $B/G$ ratio, and anisotropy elastic $A$

| Compounds | Constants | | | | | | | | | | |
|---|---|---|---|---|---|---|---|---|---|---|---|
| | $C_{11}$ | $C_{12}$ | $C_{44}$ | $B$ | $G_V$ | $G_R$ | $G_H$ | $E$ | $v$ | $B/G$ | $A_G$ (%) |
| TaCoSn | 336.77 | 109.11 | 106.87 | 185.00 | 109.65 | 109.55 | 109.60 | 274.58 | 0.25 | 1.68 | 0.04 |
| TaIrSn | 293.13 | 157.66 | 110.85 | 202.82 | 93.60 | 88.35 | 90.97 | 195.54 | 0.30 | 2.22 | 2.28 |
| TaRhSn | 270.57 | 138.75 | 80.76 | 182.69 | 74.82 | 74.08 | 74.45 | 196.64 | 0.32 | 2.45 | 0.50 |

The Poisson's ratio ($v$) is an additional parameter which describes the isotropy of a material; it is given by

$$v = (3B - 2G) / 2(3B+G) . \qquad (11)$$

The value of the Poisson coefficient that can be obtained in the case of a perfectly isotropic material is close to the Cauchy value of 0.25, thus representing a material of ionic character. The predicted values of the Poisson coefficient are respectively 0.25, 0.30 and 0.32 for TaCoSn, TaIrSn and TaRhSn respectively, which are close to 0.25, indicating that our materials are isotropic with ionic bonds. An important factor is the anisotropy factor [18] $A_G$ which measures the anisotropy of a material, defined as:

$$A_G = (G_{VOIGT} - G_{REUSS}) / (G_{VOIGT} + G_{REUSS}) . \qquad (12)$$

The material shows an elastic isotropy when $A_G$ is close to 0 % $G_{VOIGT} \approx G_{REUSS}$ , while a value of 100 % corresponds to a largest anisotropy. It is clear that the calculated factors for anisotropy presented in Table 2 are close to 0 %, confirming the isotropic nature of the compounds.

### 3.3 Electronic Properties

The electronic configurations used for the TaXSn compounds (X = Co, Ir, Rh) are [Xe] $4f^{14} 5d^3 6s^2$ for Ta, [Ar] $3d^7 4s^2$ for Co, [Xe] $4f^{14} 5d^7 6s^2$ for Ir, [Kr] $4d^8 5s^1$ for Rh and [Kr] $4d^{10} 5s^2 5p^2$ for Sn. The total (DOS) and partial (PDOS) densities of states of TaCoSn, TaIrSn and TaRhSn materials present similar shape and are shown in Fig. 1.

For all the compounds, the sharp peaks at the bottom of the valence band between about $-9$ and $-7$ eV is mainly due to the Sn 4s states. On the other hand, it is clear from the figure that the maximum contribution to the valence band is related to 3d, 5d and 4d states of Co, Ir and Rh atoms respectively, while the conduction band is mainly dominated by the Ta 5d states with a small contribution of 5d, 4d and 3d states of Rh, Ir and Co respectively.

The densities of the state's behavior near the energy gaps calculated at the points of high symmetry with other theoretical data [3] are summarized in Table 3. Our results show that all of these compounds are semiconductors with indirect band gaps of 1.08, 1.146 eV at L-X points for TaCoSn and TaIrSn respectively, and 1.145 eV at Γ-X points for TaRhSn. It can also be seen that the band structures show a flat band near the Fermi level along the Γ-L direction. These flat bands result from the rapid variation of the DOS the Fermi

level determines the thermoelectric performance of the materials.

The very large density of state values of TaCoSn, TaIrSn and TaRhSn compounds near the Fermi level play an important role in its high electrical conductivity. The calculated band structures of TaCoSn, TaIrSn and TaRhSn along the directions of high symmetry in the Brillouin zone are illustrated in Fig. 2.
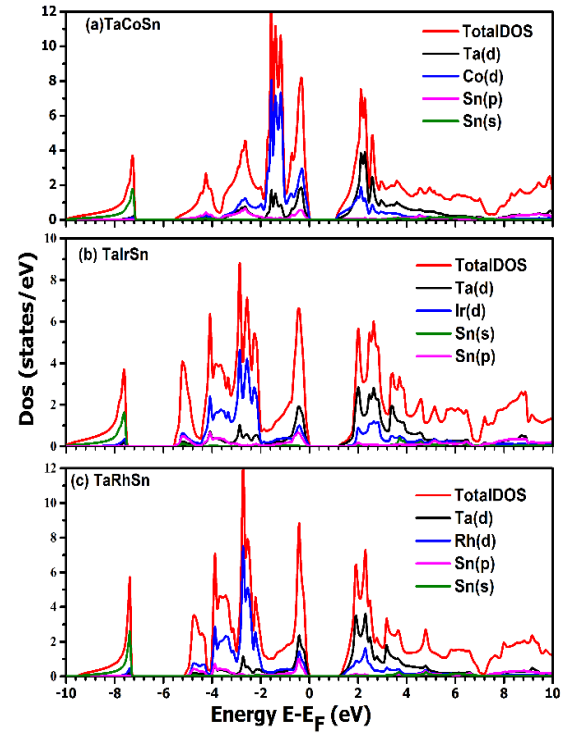


**Fig. 1** – The Total and partial densities of state calculated with TB-mBJ potential for TaCoSn (a), TaIrSn (b) and TaRhSn (c)

Which implies an effective mass of very dense electrons leading to a constitutively increase of the thermoelectric factor and consequently the thermoelectric properties.

### 3.4 Thermoelectric Properties

The three semiconductors calculated band structures suggest the presence of flat bands, which reveals good electrical transport properties. Fig. 3 illustrates the calculated thermoelectric properties of TaCoSn, TaIrSn and TaRhSn as a function of chemical potential ($\mu$) in the range energy of $-2.5$ eV to 2.5 eV at different temperatures of 300, 600 and 900 K. The undoped compound is considered for zero chemical potential ($\mu = 0$ eV) fixed in the middle of the band gap. The posi-

tive value of $\mu$ represents $n$-type doping, while the negative ones describe $p$-type doping.

### 3.4.1. Seebeck Coefficient

It is well known that for a better thermoelectric de-

vice, a high Seebeck coefficient is required. The calculated Seebeck coefficients as a function of chemical potential ($\mu$) at temperatures of 300, 600 and 900 K are shown in Fig. 3.

**Table 3** – Energy gaps in (eV) at points of high symmetry for TaCoSn, TaIrSn and TaRhSn

| Compounds | Gap type | Points of Symmetry | Gap (eV) | | |
| --- | --- | --- | --- | --- | --- |
| | | | GGA-PBEsol | TB-mBJ | Other calculations |
| TaCoSn | Direct gap | $L \rightarrow L$ | | 2.398 | |
| | | $X \rightarrow X$ | | 1.540 | |
| | | $W \rightarrow W$ | | 1.985 | 1.63[a] |
| | | $\Gamma \rightarrow \Gamma$ | | 2.5938 | |
| | | $K \rightarrow K$ | | 2.067 | |
| | Indirect gap | $L \rightarrow X$ | 1.07 | 1.08 | 1.37[a] |
| TaIrSn | Direct gap | $L \rightarrow L$ | | 2.427 | |
| | | $X \rightarrow X$ | | 1.762 | |
| | | $W \rightarrow W$ | | 2.267 | |
| | | $\Gamma \rightarrow \Gamma$ | | 3.095 | 2.26[a] |
| | | $K \rightarrow K$ | | 2.688 | |
| | Indirect gap | $L \rightarrow X$ | 0.961 | 1.146 | 1.55[a] |
| | | $\Gamma \rightarrow X$ | | 1.271 | |
| TaRhSn | Direct gap | $L \rightarrow L$ | | 2.439 | |
| | | $X \rightarrow X$ | | 1.534 | |
| | | $W \rightarrow W$ | | 2.138 | |
| | | $\Gamma \rightarrow \Gamma$ | | 2.503 | 1.76[a] |
| | | $K \rightarrow K$ | | 2.309 | |
| | Indirect gap | $\Gamma \rightarrow X$ | 1.091 | 1.145 | 1.109[b],1.40[a] |
| | | $\Gamma \rightarrow L$ | | 2.335 | |

[a] Theoretical values HSE06 [3]
[b] Theoretical values GGA-WC [19]
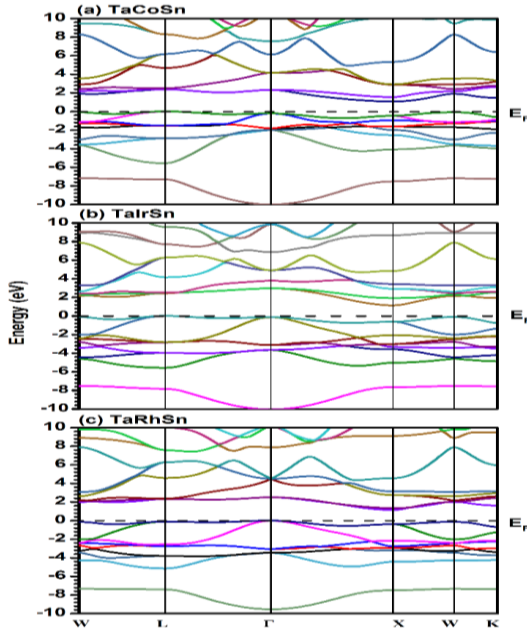


**Fig. 2** – Band structures calculated with TB-mBJ potential for TaCoSn (a), TaIrSn (b) and TaRhSn (c)

For non-doped compounds ($\mu = 0$), the values of the Seebeck coefficients $S$ are 600, 1120 and 617 µV K$^{-1}$ for TaCoSn, TaIrSn and TaRhSn, respectively. Large and positive values of $S$ lead to $p$-type doped compounds. The Seebeck coefficients are positive due to the flat valence bands along the $\Gamma$-L direction, as shown in the

band structures. The peaks are obtained between $-0.8$ and 0.6 eV, while outside this range, the curves quickly tend towards zero. We can also see that the three materials exhibit approximately the same behavior of the Seebeck coefficient and have the maximum values at 300 K. The Seebeck coefficients in the $p$-type region have the maximum values of 1820, 1930 and 1940 µV K$^{-1}$ at room temperature for TaCoSn, TaIrSn and TaRhSn, respectively, thus providing good thermoelectric properties.

Moreover, for all compounds, the equilibrium value of $S$ decreases as the temperature increases. For the $n$-type region, the maximum values of S are observed at $-1720$, $-1800$ and $-1840$ µV K$^{-1}$ for TaCoSn, TaIrSn and TaRhSn, respectively, which are lower than those of the $p$-type. Thus, $p$-type doping, TaCoSn, TaIrSn and TaRhSn materials give better thermoelectric performance.

### 3.4.2. Electrical Conductivity

Fig. 4 illustrates the calculated electrical conductivities $\sigma/\tau$ (where $\tau$ is the relaxation time in seconds) as function of the chemical potential ($\mu$) at temperatures of 300, 600 and 900 K for the three compounds. Note that the shape of the representative curves is similar at given temperatures and $\sigma/\tau$ increases with $\mu$ in the same way for all temperature values. An increase in $\mu$ is affected by increasing the carrier concentration, leading to high conductivity.
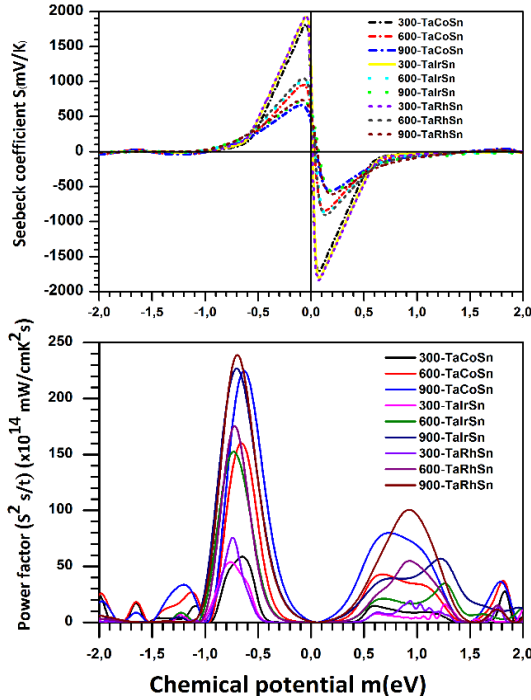
**Fig. 3** – Seebeck coefficients $S$ ($\mu$V K$^{-1}$) and power factor as a function of chemical potential $\mu$ at temperatures of 300, 600, and 900 K for TaCoSn, TaIrSn and TaRhSn

Electrical conductivity has a greater value for negative than positive $\mu$, indicating that $p$-type doped compounds have higher conductivity than $n$-type doped ones. Between about $-0.50$ and 0.60 eV, the electrical conductivities are zero for $p$-type and $n$-types doped compounds, beyond these points, the electrical conductivity increases where TaCoSn, TaIrSn and TaRhSn compounds can provide the best thermoelectric properties. In addition, the maximum calculated values of the electrical conductivities at $-0.95$ eV are $3.69 \times 10^{20}$ $\Omega^{-1}$m$^{-1}$s$^{-1}$, at $-1.07$ eV is $3.96 \times 10^{20}$ $\Omega^{-1}$m$^{-1}$s$^{-1}$ and at $-1.02$ eV is $3.71 \times 10^{20}$ $\Omega^{-1}$m$^{-1}$s$^{-1}$ with positive doping for TaCoSn, TaIrSn and TaRhSn, respectively.

### 3.4.3. Thermal Conductivity

As mentioned above, a low thermal conductivity is necessary to obtain a good material for thermoelectric technology. The variation of the thermal conductivity ($K_{el}/\tau$) with respect to the chemical potential ($\mu$) at different temperatures of 300, 600 and 900 K of TaCoSn, TaIrSn and TaRhSn compounds is depicted in Fig. 4. It is easily observed that $K_{el}/\tau$ increases with $\mu$ for all temperatures. On the other hand, the thermal conductivities are zero between $-0.55$ and 0.60 eV for TaCoSn, $-0.60$ to 0.75 eV for TaIrSn and $-0.60$ to 0.75 eV for TaRhSn over the whole temperature range. In these regions, our materials are expected to provide thermoelectric devices with very good performance. Outside these ranges of chemical potential, a considerable increase is observed in the electronic thermal conductivities of these compounds.

At 300 K and for $p$-type doping, the thermal conductivity reaches peak values of $24.16 \times 10^{14}$, $27.41 \times 10^{14}$
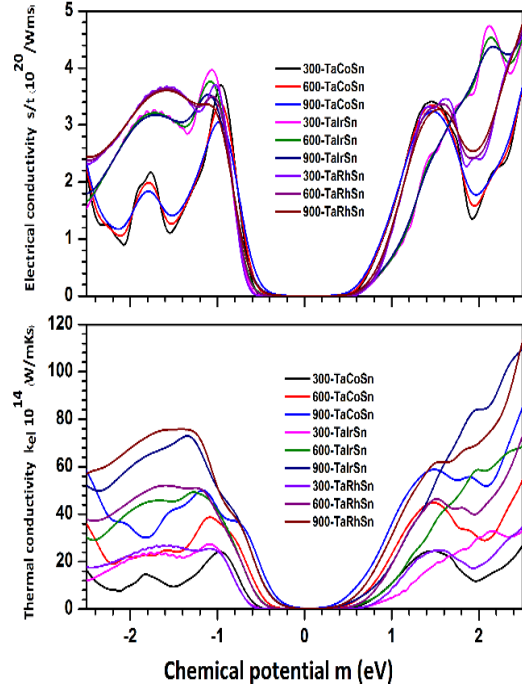


**Fig. 4** – Electrical conductivity $\sigma/\tau$ ($10^{20}$/$\Omega$·m·s) and thermal conductivity $K_{el}/\tau$ ($10^{14}$ W/mK s) for TaCoSn, TaIrSn and TaRhSn at temperatures of 300, 600 and 900 K

and $25.51 \times 10^{14}$ W K$^{-1}$m$^{-1}$s$^{-1}$ for TaCoSn, TaIrSn and TaRhSn, respectively.

### 3.4.4 Figure of Merit

The figure of merit (ZT) reflects the performance of a thermoelectric material, which is related to the Seebeck coefficient, electrical conductivity and thermal conductivity by the following relationship:

$$ZT = \sigma S^2 T / K, \tag{13}$$

where $\sigma$ is the electrical conductivity, $S$ is the Seebeck coefficient, $T$ is the temperature and $\kappa$ is the thermal conductivity.

Materials are considered good elements for thermoelectric devices if their ZT is greater than or equal to unity [20]. The ZTs as a function of chemical potential at different temperatures of 300, 600 and 900 K for TaCoSn, TaIrSn and TaRhSn are displayed in Fig. 5. It can be noted that the ZTs of all these materials are very close to unity at room temperature, which reveals that the materials TaCoSn, TaIrSn and TaRhSn are promising candidates for thermoelectric applications.

The figure of merit varies sharply in the vicinity of 0 eV and the peak values are observed between $-0.30$ and 0.16 eV for TaCoSn, from $-0.15$ to 0.15 eV for TaIrSn and from $-0.17$ to 0.15 eV for TaRhSn. Indeed, in these ranges, the thermal conductivity is almost zero and the Seebeck coefficient reaches the maximum value. Finally, ZT vanishes when the chemical potential exceeds 1.50 eV in the $p$-type region for all materials, which it is obvious since in this region the electrical conductivity is zero.
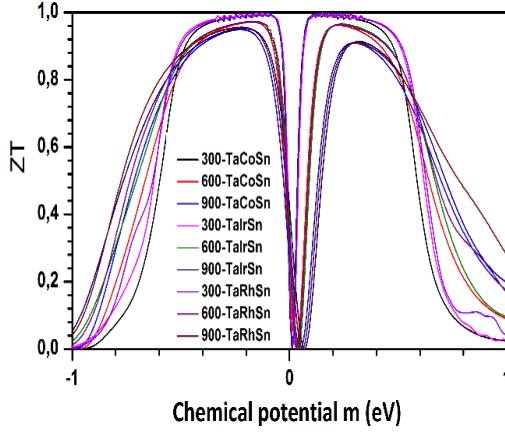
**Fig. 5** – Figure of merit (ZT) as a function of chemical potential ($\mu$) at temperatures of 300, 600 and 900 K for TaCoSn, TaIrSn and TaRhSn

### 3.4.5. Thermopower Factor and Optimal Doping

The thermoelectric performances of a material are also evaluated by its thermoelectric power factor defined with respect to the relaxation time as ($S^2\sigma/\tau$). This factor must have important values to improve the electric transport properties in order to obtain excellent thermoelectric materials. As we have seen, the Seebeck coefficient $S$ is higher for negative values of $\mu$, implying that $p$-type doping will provide better thermoelectric behavior compared to $n$-type doping for these compounds, this result prompt us to study the doping of these materials in order to determine the optimal doping level leading to maximum thermoelectric power factors for the TaCoSn, TaIrSn and TaRhSn materials. To reach this goal, we calculated the Seebeck coefficient

and electrical conductivity as a function of different doping concentrations in the range of $10^{19}$ to $2.41 \times 10^{22}$ cm$^{-3}$ for the $n$- and $p$-type doping levels with a $0.1 \times 10^{19}$ cm$^{-3}$ doping pitch.
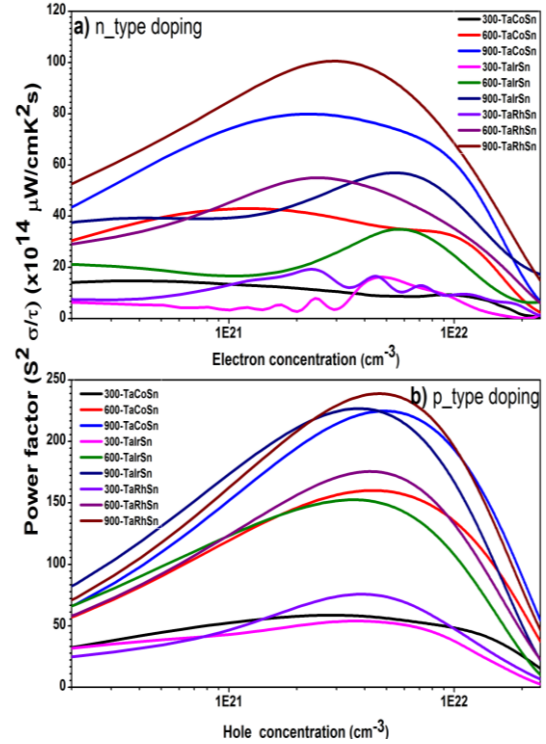


**Fig. 6** – Variations of the thermoelectric power factor $S^2\sigma/\tau$ ($10^{14}$ µW/cm K$^2$ s) as a function of the carrier concentration (carrier/cell unit) at temperatures of 300, 600 and 900 K for TaCoSn, TaIrSn and TaRhSn, $n$-type (a), $p$-type (b) doping

**Table 4** – Thermoelectric power factor $S^2\sigma/\tau$ ($10^{14}$ µW/cm K$^2$ s) and corresponding optimal doping level (carrier/cell unit) for the $p$- and $n$-type doping, temperatures of 300 K, 600 K and 900 K for TaCoSn, TaIrSn and TaRhSn

|  | Temperature | $p$-type doping | | $n$-type doping | |
|---|---|---|---|---|---|
|  |  | Doping level | Power factor | Doping level | Power factor |
| TaCoSn | 300 | 0.149519 | 058.69 | 0.0210663 | 14.78 |
|  | 600 | 0.221453 | 160.13 | 0.0621714 | 42.97 |
|  | 900 | 0.252282 | 224.78 | 0.1186909 | 79.89 |
| TaIrSn | 300 | 0.2192254 | 053.95 | 0.278315 | 16.21 |
|  | 600 | 0.2133164 | 152.57 | 0.337406 | 34.90 |
|  | 900 | 0.2251345 | 226.78 | 0.325588 | 56.94 |
| TaRhSn | 300 | 0.2259361 | 075.76 | 0.13348144 | 19.31 |
|  | 600 | 0.2432713 | 175.60 | 0.14503827 | 55.01 |
|  | 900 | 0.2663850 | 238.92 | 0.16815194 | 100.57 |

The variations of the thermoelectric power factors as a function of the concentrations of the charge carriers at temperatures 300, 600 and 900 K are plotted in Fig. 6 for the $p$-type doping and $n$-type doping. Table 4 summarizes the maximum calculated factors with the corresponding optimal doping levels for the materials TaCoSn, TaIrSn and TaRhSn. It is clear that the peak values of these factors are more important for the $p$-type doping compared to $n$-type doping; this is probably due to the high density of states at the maximum of the valence band where the electrical conductivity has a high value, unlike the conduction band where the density of states is lower.

In addition, it can be seen that thermoelectric pow-

er increases with increasing temperature and TaRhSn compounds has the highest power factor for the whole temperature range and we can say that $p$-type doping gives the highest values of the power factor of $53.95 \times 10^{14}$ µW cm$^{-1}$·K$^{-2}$·s$^{-1}$ at 300 K for the TaIrSn and up to $238.92 \times 10^{14}$ µW cm$^{-1}$·K$^{-2}$·s$^{-1}$ at 900 K for TaRhSn.

### 4. CONCLUSIONS

By using FP-LAPW method with the GGA-PBEsol approximation and applying the TB-mBJ potential, we calculated the structural, electronic, elastic and thermoelectric properties of TaCoSn, TaIrSn and TaRhSn.

These materials are found to be mechanically stable semiconductors in the LiAlSi type cubic structure, ductile and isotropic with ionic bonds. The three TaCoSn, TaIrSn, and TaRhSn compounds have an indirect band gap of 1.08, 1.146, and 1.145 eV, respectively. We have found that the maximum power factor is given by the TaRhSn compound with *p*-type doping. Moreover, the results of the optimal doping level show that high thermoelectric powers are given by TaXSn (X = Co, Ir, and Rh) wit *p*-type doping. Therefore, TaCoSn, TaIrSn and TaRhSn semiconductors are predicted to be perfect candidates for thermoelectric applications.

## REFERENCES

1. H. Alam, S. Ramakrishna, *Nano Energy* **2**, 190 (2013).
2. R.J. Mehta, Y.L. Zhang, C. Karthik, B. Singh, R.W. Siegel, T. Borca-Tasciuc, G. Ramanath, *Nat. Mater.* **11**, 233 (2012).
3. R. Gautier, X. Zhang, L. Hu, L. Yu, Y. Lin, T.O.L. Sunde, D. Chon, K.R. Poeppelmeier, A. Zunger, *Nat. Chem.* **7**, 308 (2015).
4. G.K.H. Madsen, D.J. Sing, *Comput. Phys. Commun.* **175**, 67 (2006).
5. E. Sjöstedt, L. Nordström, D.J. Singh, *Solid State Commun.* **114**, 15 (2000).
6. P. Blaha, K. Schwarz, GKH. Madsen, D. Kvasnicka, J. Luitz, *Wien2k, An Augmented Plane Wave + Local Orbitals Program for Calculating Crystal Properties* (Universitat Wien, Autriche: Karlheniz Schwarz, Techn: 2001).
7. J.P. Perdew, A. Ruzsinszky, G.I. Csonka, O.A. Vydrov, G.E. Scuseria, L.A. Constantin, X. Zhou, K. Burke, *Phys. Rev. Lett.* **100**, 136406 (2008).
8. F. Tran, P. Blaha, M. Betzinger, S. Blügel, *Phys. Rev. Lett.* **102**, 226401 (2009).
9. H.J. Monkhorst, J.D. Pack, *Phys. Rev. B.* **13**, 5188 (1976).
10. J.D. Pack, H.J. Monkhorst, *Phys. Rev. B.* **16**, 1748 (1977).
11. F.D. Murnaghan, *P. Natl. Acad. Sci. USA* **30**, 244 (1944).
12. J. Heyd, G.E. Scuseria, M. Ernzerhof, *J. Chem. Phys.* **118**, 8207 (2003).
13. H.S. Chen, *Anisotropy of Elasticity about Metal* (Beijing: Metallurgy Industry Press: 1996).
14. R.E. Newnham, *Properties of Materials, Anisotropy, Symmetry, Structure.* (New York USA: Oxford University Press: 2005).
15. R. Hill, *P. Phys. Soc. A* **65**, 349 (1952).
16. J.H. Wang, S. Yip, S.R. Philpot, D. Wolf, *Phys. Rev. Lett.* **71**, 4182 (1993).
17. S.F. Pugh, *Philos. Magn.* **45**, 823 (1954).
18. D.H. Chung, W.R. Buessem, *In Anisotropy in Single-Crystal Refractory Compounds.* **2**, 217 (New York: Plenum Press: 1968).
19. D.H. Hoat, *Comp. Mater. Sci.* **159**, 470 (2019).
20. T. Takeuchi, *Mater. Trans.* **50**, 2359 (2009).